



Physical and Mechanical Behaviours of Tympanotonus Fuscatus Reinforced Polyethylene

Victoria Dumebi OBASA¹, Samuel OKONKWO³, Oludolapo Akanni OLANREWAJU², Samson Oluropo ADEOSUN^{2,3}, Olugbemi OMOTOSO³, Adebola OMOOLORUN³

¹Department of Industrial and Production, Lagos State University, Lagos, Nigeria
victoria.obasa@lasu.edu.ng

²Department of Industrial Engineering, Durban University of Technology, Durban 4000, South Africa
Oludolapo0@dut.ac.za

³Department of Metallurgical and Materials Engineering, University of Lagos, Lagos 101017, Nigeria
sammypaco@gmail.com/sadeosun@unilag.edu.ng/olugbemiotomoso@gmail.com/omoolorunadebola1@yahoo.com

Corresponding Author: victoria.obasa@lasu.edu.ng, +2348065483727

Date Submitted: 06/06/2024

Date Accepted: 07/04/2025

Date Published: 11/04/2025

Abstract: This paper investigated the physical and mechanical characteristics of the periwinkle shell (*Tympanotonus fuscatus*) particle to determine its effectiveness as reinforcement in polyethylene matrix composite for potential engineering applications with a reduction in fossil-based constituents with its attendant environmental impact. The composites were constituted from periwinkle particle fractions from 5 to 40 wt. %, with five different particle sizes: 106, 150, 177, 250, and 420 μm . Test specimens were investigated via Fourier Transform Infrared Spectroscopy (FTIR), Scanning Electron Microscopy (SEM), X-ray diffraction (XRD), tensile, impact, and flexural, density, and water absorption evaluations. Results showed that densities of samples at all particle sizes increased with filler content but reduced with enlargement of the particle size of the filler owing to the increase in void sizes between the filler and the matrix. However, the developed composites still feature within the density range of low-density, to linear low-density of polymer composite. The water absorptivity decreased as the filler content increased due to the crystalline nature of the filler. Specifically, composites' peak impact energy, and flexural strength, of 21.54 J for 150 μm sample at 40 wt. % filler content and 11.96 MPa for 106 μm sample at 5 wt. % filler content was recorded respectively. FTIR spectrum shows the presence of additional C=C and C-O-C groups. Also, SEM micrographs indicated strong interfacial bonding between the filler and the matrix, and good filler dispersion in the matrix, which accounted for relative improvement in mechanical properties. Hence, the developed periwinkle particulate-reinforced low-density polyethylene composite can be used for decorative purposes or in car interior design where high strength is not a critical requirement.

Keywords: Low-density Polythene, Composite, Filler, Periwinkle, Physical Properties

1. INTRODUCTION

Studies on polymer-based composites have evolved over the years providing alternate routes for formulations of composites with optimal properties for special applications like automotive, aerospace and defence, construction, marine, and oil and gas [1,2]. Natural fibre-reinforced composites are gaining prominence over synthetic reinforced composites due to their low cost, renewability, low density, high strength, and biodegradability. Significant progress has been recorded in developing composite with enhanced properties using various agro-waste fillers reputed for environmentally friendliness as reinforcing agents with the polymers as matrixes [3]. Multicomponent fillers comprising cellulose, hemicellulose, and lignin, are being investigated for their suitability to replace synthetic fibres [4,5]. In developing economies, harvest seasons are accompanied by abundant agricultural waste that constitutes an environmental menace. In Nigeria, the extent of fishing activities in the coastal areas leads to large volumes of sea shells which are left as waste after consumption of the fleshes of these species as protein. These shells constitute environmental pollution as they are dumped around open sites. [6]. Examples of sea shells are remains of aquatic animals like periwinkles, crabs, prawns, etc.

Periwinkle or winkle (*Turritella communis*) is small shore-dwelling mollusca with a hard spiral shell. It is a comestible class of sea snail of the aquatic gastropod Mollusca [7]. It possesses an outer skeleton, which protects it from predators and mechanical damage. The shell has several layers with an organic matrix (conchiolin) bonded with calcium carbonate precipitates. The CaCO_3 robust shell is hard and impermeable to water making it a potential material for wide engineering applications [8]. Hence, this work explored the conversion of this potential waste product- Periwinkle shell into useful raw material. An earlier study found that sea shells like periwinkles have satisfactory compressive properties in concrete and can serve as fractional or full replacements for granite in concrete [9]. These residual materials could be harnessed,

transformed, and utilized in developing a new set of materials for use in a varied application. The combination of strength and resistance to water absorption by periwinkle shell could be utilized in polymeric materials in the transportation industry not only for lightness but also for resistance to degradation by moisture. Previous studies on the use of periwinkle shell-reinforced polymer recorded high flexural and compressive strength but low tensile strength consequent on the brittle nature of the reinforcement [10, 11]. Other complementary work, which made use of natural fillers such as coconut fibre, palm kernel shell coir fibre reported high flexural modulus, and compressive strength but low compressive strength [12,13]. Due to the low values of ultimate tensile strength (UTS), the composite developed from these found its application in areas where high strength is not a major criterion.

Periwinkle shell is chosen over other sustainable reinforcement options due to the need to valorize waste into useful economic materials and consequently to its unique properties as highlighted. Periwinkle shells are distinctive as a natural filler due to their greater hardness, density, and abrasion resistance compared to coconut fibre and palm kernel shell. Their calcium carbonate composition provides enhanced mechanical properties, thermal stability, and durability in composites. Unlike fibrous alternatives, they are less susceptible to degradation and offer versatile applications in bioplastics, concrete reinforcement, and abrasives. Furthermore, they are an eco-friendly byproduct of the seafood industry, making them a sustainable option.

Deductions from the literature have shown that naturally reinforced polymers are notable for low strength when compared with synthetic counter parts (carbon and glass fibres) but are useful in non-structural applications for example roof tiles, panels for partitions, windows, false ceilings, and door frames with lightweight, low strength requirement. This study is thus aimed at examining the potential utilization of periwinkle shell (pulverized) as a reinforcing material in polyethylene composites for engineering applications [10,14,12].

2. MATERIALS AND METHODOLOGY

2.1 Materials

The periwinkle shell used for this investigation was purchased from a local vendor in Bariga area of Lagos State, Nigeria. The periwinkle shell was dried in the sun for three days consecutively thereafter it was pulverized at the Federal Institute of Research Oshodi (FIRO), Lagos State, Nigeria. In its milled state, the periwinkle shell was sieved into five different particle sizes (420, 250, 177, 150, and 106 μm) in the Department of Metallurgical and Materials Engineering Laboratory of the University of Lagos, Nigeria. Both the filler (periwinkle) and the LDPE were weighed appropriately using a weighing balance. For this work, the weight of the filler (periwinkle shell) was varied from 5 to 40 wt. % (in step 5) of the initial mass of the LDPE. This process was repeated for the five different particle sizes. A rectangular wooden pattern with six cavities each for hardness, impact, tensile, and flexural samples was used as the casting mould. The periwinkle shell and low-density polyethylene (LDPE) in their appropriate weight were then charged into a stir casting machine, heated to 135°C, and discharged into the wooden cavities coated with paper tape. The paper tape protects the mould surface from interaction with the discharged composite and acts as a releasing agent. The molten polymer composites were allowed to cool in the wooden cavity to room temperature.

2.2 Measurement of Physical Properties

The density of each cast composite was estimated as ratio of the sample mass to its volume. To determine the composites' water absorption behaviour, the weight of developed composites was taken before immersion into distilled water at 32°C for 5 days. After which they were removed, gently cleaned with a soft cloth to eliminate excess water, and then weighed again. The percentage absorption (ABS %) of LDPE composites was further calculated in terms of the measured weights W_b and W_a using Equation 1, where W_b and W_a are weights before and after immersion represented

$$ABS (\%) = \frac{W_a - W_b}{W_b \times 100} \quad (1)$$

2.3 Evaluation of Mechanical Behaviours

This flexural test, tensile and impact were done in the Department of Materials Science and Engineering, Obafemi Awolowo University, Ile-Ife, Osun State, Nigeria. Using a dumbbell test piece, the tensile test was done according to ASTM D7264 standard procedure. The specimens were tested at a crosshead speed of 20 mm/min.

2.4 Structural Analysis

A SHHIMADZU FTIR-8400 S spectrometer located at Redeemers University, Ede, Nigeria was used in carrying out FTIR spectra of samples in transmission mode. Ten milligrams of fine samples were dispersed in a matrix of KBr (500 mg), followed by compression at 22–30 MPa to form pellets. The transmittance measurements were carried out between 400–4000 cm^{-1} at a resolution of 4 cm^{-1} .

2.5 Crystallographic Analysis

The X-ray diffractometry was determined on an EMPYREAN XRD-6000 diffractometer using Cu, $K\alpha$ radiation ($\lambda=1.540598\text{nm}$, Ni-filter) at 40 kV, 30 mA. The samples lacking preferred orientations were scanned in steps of 0.026261 in the 2θ range from 4.99 to 75 using a count time of 29.7s per step. Crystallinity index (CrI) for periwinkle was calculated using Equation 2 [15,16].

$$Crl(\%) = \left(\frac{I_c}{I_c + I_a} \right) \times 100 \tag{2}$$

where I_c and I_a represent the intensities of the crystalline and amorphous region respectively.

2.6 Morphological Analysis

The sample images were captured by a SEM model Phenom Eindhoven, Netherlands. It uses an electron intensity beam of 15 kV, and the specimens for observation are mounted on a conductive carbon imprint left by the adhesive tape. This is often prepared by inserting the specimen into the circular holder and then coated for 5 min to enhance its electrical conductivity. The microstructure examination of the samples was carried out at the Mechanical Engineering laboratory at Covenant University Nigeria.

3. RESULTS AND DISCUSSION

3.1 Functional Group Analysis of Periwinkle Shell

FTIR spectroscopy of virgin periwinkle shell gave vital information about its structure and absorptive characteristics. Absorption bands observed between 4000 to 500 in the FTIR spectra (Figure 1) revealed functional peaks at 1798, 1420-1430, and 876 consistent to out-of-plane bending and asymmetrical stretching vibration peaks of O–C–O typical of calcite (CaCO_3) [17]. But it is devoid of adsorption bands at 2924–2872 of C–H of stearic acid usually present in FTIR spectra of calcite when compared with the work of Hajji *et al.* (2017) [18]. This suggests that the type of calcium carbonate present in periwinkle shells has minimal absorptive properties hence it can enhance the properties of polymer composites by improving its stiffness, strength, and thermal stability [19].

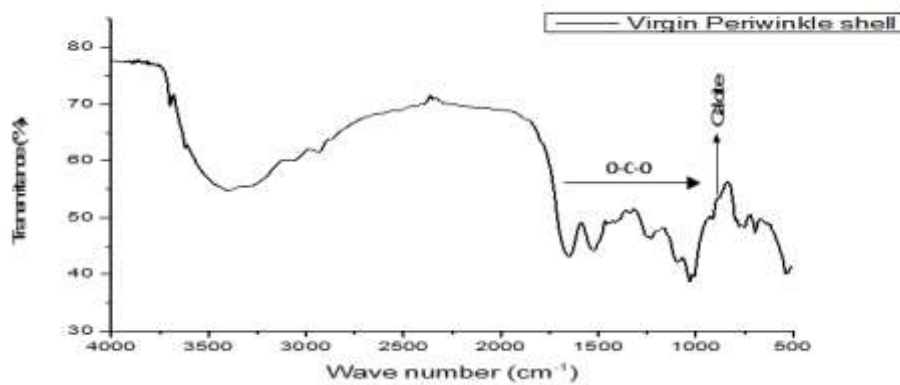


Figure 1: FTIR spectrum of virgin periwinkle shell

3.2 Functional Groups Analysis of LDPE

The FTIR spectrum of unreinforced LDPE lies within 4000 and 500 cm^{-1} and the report of the identified functional groups is shown in Figure 2 and Table 1 respectively. The typical absorbance at 3439 cm^{-1} implies OH bending. Strong CH_2 and weak CH_3 symmetric stretching occurs at 2860 and 1377 cm^{-1} respectively while as symmetric stretching and bending of CH_2 is absorbed at 2918 and 1464 cm^{-1} respectively. The twisting deformation of CH_3 is absorbed at 1301 cm^{-1} , but with weak intensity. The group also reveals a rocking deformation of medium intensity at 719 cm^{-1} . This spectrum conforms with the observation of Morsch *et al.* [20] for the main band of LDPE in the IR characterization. In addition to their findings, the presence of weak symmetric deformation of CH_3 at 1377 cm^{-1} is a typical feature of low-density polyethylene (LDPE). A weak asymmetric mode of the carbonyl group ($\text{C}=\text{O}$) exists at 1720 cm^{-1} and this is similar to LDPE spectrum investigated by Shivasharana & Sheetal [21].

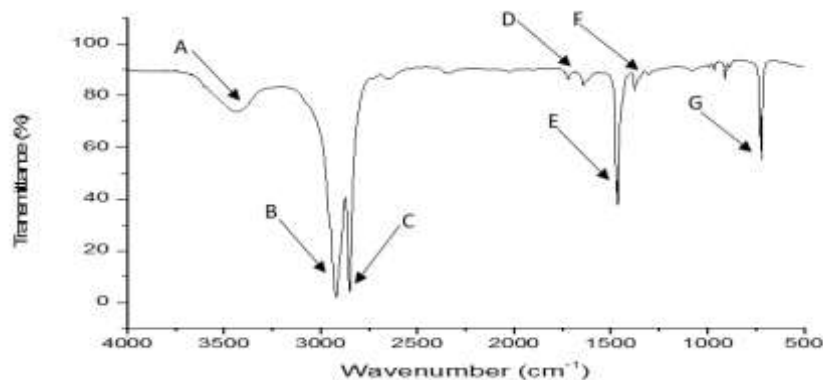


Figure 2: FTIR spectrum of LDPE

Table 1: Description of functional group

Position	Wave Number (cm ⁻¹)	Functional Group
A	3439	OH bending
B	2918	Asymmetric stretching CH ₂
C	2860	Strong CH ₃ symmetric stretching
D	1720	Weak Asymmetric carbonyl group (C=O)
E	1464	Asymmetric bending CH ₂
F	1377	Weak CH ₃ symmetric stretching
G	719	Alkanes/Alkenes C-H Bend (Rocking deformation of medium intensity)

3.3 The Crystallinity Behaviour of Periwinkle Shell Extract

The crystallinity of the virgin periwinkle shell as determined by XRD spectral analysis is shown in Figure 3. The observed spectra have very sharp peaks indicating that the periwinkle shell is crystalline in nature. Diffraction peaks occurred at 27.07°, 35.84°, 42.72° which matches that of calcite [16]. The presence of calcium carbonate (CaCO₃) in periwinkle shells can have both enhancing and diminishing effects on the characteristics of a polymer composite, dependent on several factors such as the concentration, distribution, and interaction between the filler and the polymer matrix. This will be further ascertained by other investigation reported in the following section.

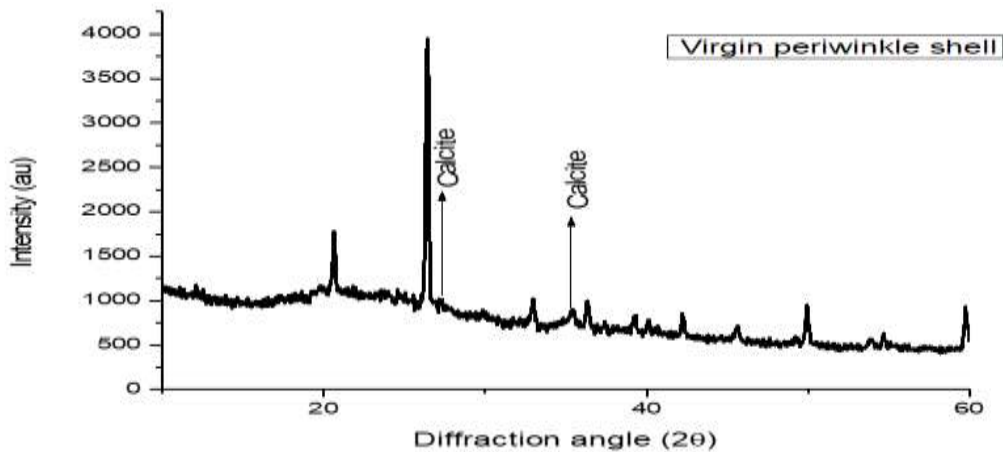


Figure 3: XRD spectra of virgin periwinkle shell

3.4 The Density Evaluation of the Polymer Composites

The plot of density against filler content as shown in Figure 4 revealed that densities of all particle sizes increased gradually from 5 wt.% filler contents until 20 wt.% after which a wavy pattern developed from 25 to 40 wt. %. Ibrahim *et al.* (2015) [22] did not observe this wavy pattern as his investigation was limited to 5 to 20 wt.% filler contents. A careful analysis of the graphs showed that the density of the polyethylene composite increases, with every decrease in the particle size in congruence with the study of Abutu *et al.* [23]. This occurrence can be attributed to a reduction in voids within the matrix. Notably, for all particle sizes considered the variation in density is quite minimal, especially at lower filler concentrations applicable for polymer-based lightweight composite materials suitable for industry requirements [24]. Deduction from this study shows a marginal value of densities with the highest being 1.42 g/cm³ at 106 μm for 20 wt.% filler and 0.69 g/cm³ at 420 μm, 5 wt.% filler samples. This can be related to the crystallinity of the reinforcement (Periwinkle shell). Generally, amorphous polymers are notable for a random molecular structure. This translates into lower density due to the unsystematic prearrangement of the chains, while crystalline polymers possess a systematic and regular ordering of polymer chains and crystals resulting in their high density.

3.5 Water Absorptivity of Polymer Composites

Generally, it can be seen in Figures 5a to 5e that the level of water absorption of the composite decreases as filler content increases, this aligns with the study of Ibrahim *et al.* (2015) [22] on particle board production using periwinkle shells ash-reinforced composite. However, this prediction does not agree with Adeosun *et al.*'s (2015) [25] work on coconut shells reinforced composite consequent on the hydrophilic nature of the reinforcing particles. In contrast, periwinkle shell is a hydrophobic inorganic material and does not have a strong affinity for water absorption. (Davies *et al.*, 2022) [26]. The absence of water functional groups will also decrease the composite's water absorption. It can also be seen from the chart that for each particle size, as the immersion time increases, the water absorption property increases. The highest water absorption value of 25.39 % was attained by the 106 μm at 5 wt. % filler after soaking for 3 days while water absorption of 0.91% was observed at the 40 wt. % filler after soaking for 1 day. The water transport through these

composites could be ascribed to the magnitude of voids present in the matrix owing to filler sizes used as reinforcement in the polyethylene matrix [27,28].

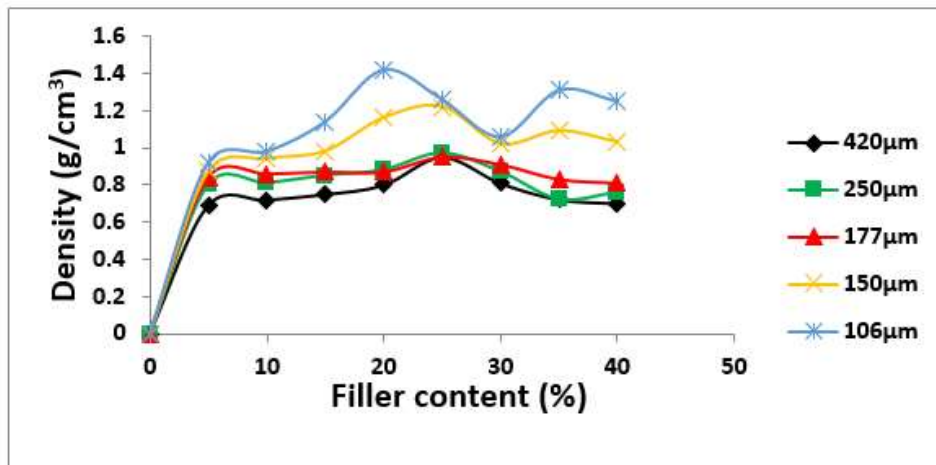


Figure 4: Polyethene composites' density (g/cm^3) with filler content for all particle sizes

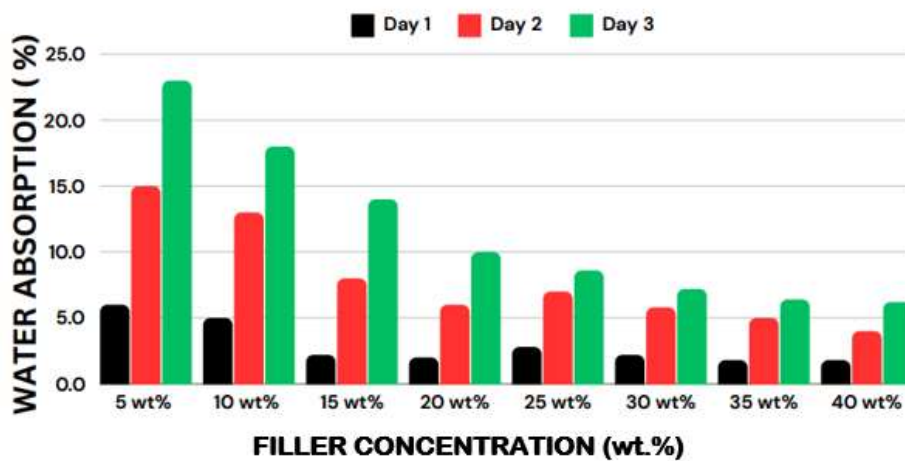


Figure 5a: Absorptivity of polyethene composite with 420 µm grade periwinkle shell

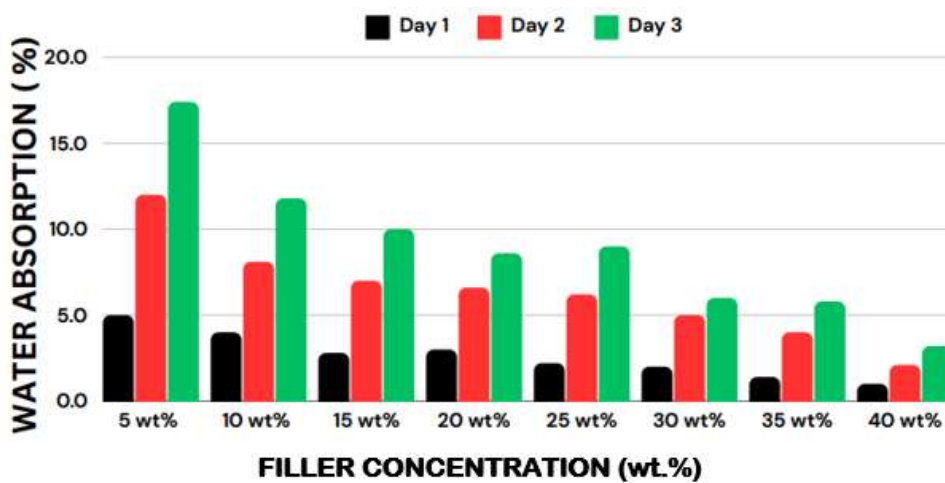


Figure 5b: Absorptivity of polyethene composite with 250 µm grade periwinkle shell

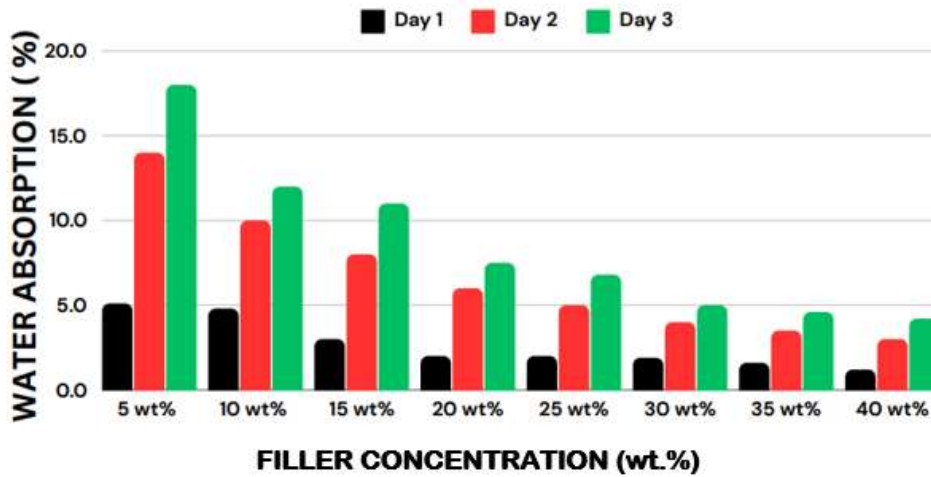


Figure 5c: Absorptivity of polyethene composite with 177 μm grade periwinkle shell

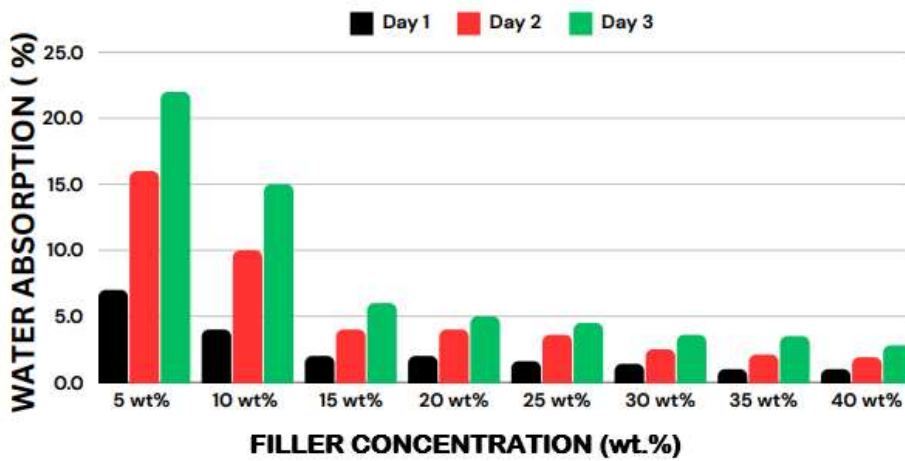


Figure 5d: Absorptivity of polyethene composite with 150 μm grade periwinkle shell

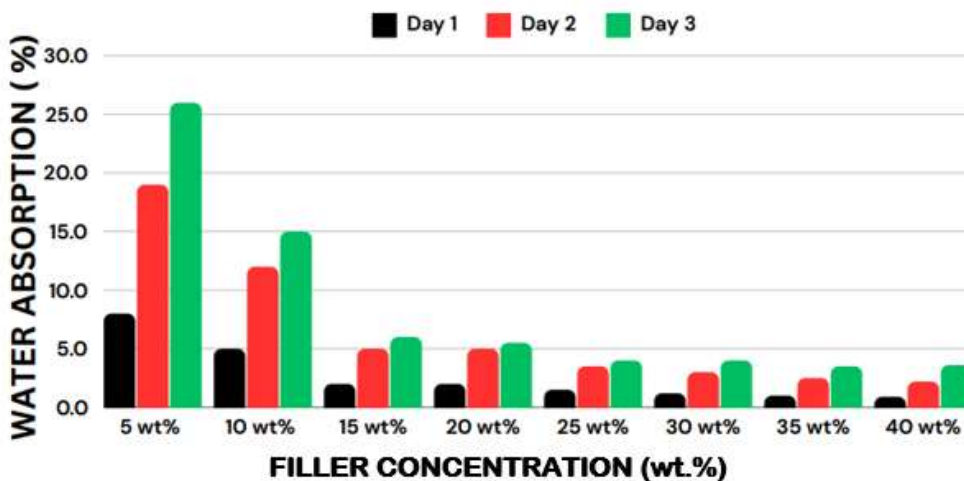


Figure 5e: Absorptivity of polyethene composite with 106 μm grade periwinkle shell

3.6 Statistical Analysis of Composite Absorptivity

3.6.1. Analysis of variance (Two-Factor ANOVA)

The need to establish the interplay amongst various parameters of soaking time, filler concentration, and particle size on composite absorptivity necessitated a comprehensive statistical analysis. A variance analysis (ANOVA) adopted in this study provided information about the significance level of the various factors on the dependent variable. A null hypothesis H_0 : $\mu_1 = \mu_2 = \mu_3 = \mu_4$ (indicative of no variance in mean) and alternate hypothesis H_1 : implying a variation in

mean at the level of significance $\alpha = 0.05$ were set up following the assumption of the Shapiro-Wilk test [29]. The total variation was further partitioned into model one and model two. Model one considered the effect of filler concentration, particle size, and their combined effect on composite water absorptivity. While, model two further examined the effect of soaking time, particle size, and their interactions. The results of the ANOVA analysis as shown in Tables 2 and 3 were generated using Statistical Kingdom computing software.

In Table 2, model one evaluates the possibility of substantial variance in the mean of the 8 cells (cells are defined by filler concentration and particle size). The F statistic value 36.791 obtained in model one test is large and greater than the F- critical value 2.31 indicating that the variance between the sample means of this group is sufficiently large to be statistically significant. The $1.502e-13$ suggests that the chance of a type 1 error is small. Since $p\text{-value} < \alpha$, H_0 is rejected. The preceding deduction calls for further analysis to ascertain the remote effect of concentration, particle size (A), and also combined effect of their interaction. Considering the effect of the particle size, the P-value of $0.3909 > \alpha$ and F-statistics $1.0419 < F\text{-critical } 2.49$ indicates that the difference between the sample averages of all groups is not large enough to be statistically significant hence, H_0 cannot be rejected. By implication, though particle size affects the absorptivity of the composite, the impact is minimally small to be significant. Further analysis of factor B (filler concentration) produced a P-value $1.406e-12 < \alpha$ and F-statistics $15.359 > F\text{-critical } 2.13$ in favour of the adoption of H_1 and rejection of H_0 . This implies that filler concentration has a significant impact on the water absorption of the composite. The P-value $0.999 > \alpha$ and F-statistics $0.332 < F\text{-critical } 1.617$ for the combined factors shows that interaction between AB does not significantly affect the composite's water absorption. Hence the null hypothesis H_0 cannot be rejected.

Table 2 relates the remote effect of soaking time, particle size, and their interactions (combined effect). The P- value 0.00000127 and F- statistics 51.7 of model two show a significant relationship between the mean of the two factors under consideration hence, H_0 is rejected while upholding H_1 . The P-value 0.5406 and F- statistics 0.78 obtained for factor A (particle size) describe a medium impact of particles on water absorption of the composite. Factor B soaking time with a P – value $3.35e - 8$ and F-statistics 20.4 call for rejection of H_0 and validation of H_1 . By implication, soaking time significantly affects the magnitude of water absorbed by the composite. The interaction between the two did not attain statistical significance with a P-value of 0.9901 and F-statistics of 0.201. Hence H_0 cannot be rejected. This means that the interaction between the two factors has no significant effect on the water absorption of the composite.

Table 2: Two-way ANOVA table for model one

Source of Variation	Degrees of freedom (df)	Sums of Squares (SS)	Mean Squares (MS)	F-Statistics	F- Critical	P-Value
Model One	7	554.005	79.144	36.791 (7,32)	2.31	1.502e-13
Factor A (Particle size μm)	4	63.575	15.894	1.0419 (4,80)	2.49	0.3909
Factor B (Concentration Wt.%)	7	1640.051	234.293	15.359 (7,80)	2.13	1.406e-12
Interaction AB	28	141.621	5.0579	0.332 (28,80)	1.617	0.9992
Residual/Error	105	2139.2587				
Total	119	3065.5732				

Table 3: Two-way ANOVA table for model two

Source of Variation	Degrees of freedom (df)	Sums of Squares (SS)	Mean Squares (MS)	F-Statistics	F- Critical	P-Value
Model Two	2	103.746	51.873	51.69 (2,12)	3.89	0.00000127
Factor A (Particle size μm)	4	63.5753	15.8938	0.78 (4,105)	2.46.	0.5406
Factor B (Soaking Time)	2	829.9715	414.9858	20.37 (2,105)	1.50	3.35e-8
Interaction AB	8	32.7677	4.096	0.20 (8,105)	2.03	0.9901
Error	105	2139.2587				
Total	119	3065.5732				

3.6.2. Mean-variance analysis of composite water absorptivity

The mean analysis of model one in Figure 6a shows that water absorption decreases with increasing filler concentration. While the water absorption showed minimal and inconsistent variation with increasing particle size. Figure 6b is a plot of mean time to water absorption for the various filler concentrations (model two). Similar to the reported observation in model one, the level of water absorption decreased significantly with increasing filler concentration. Also, the mean plot shows a consistent increment in water absorption with increasing soaking time. These inferences implied that both factors; soaking time and filler concentration have a significant effect on water absorption.

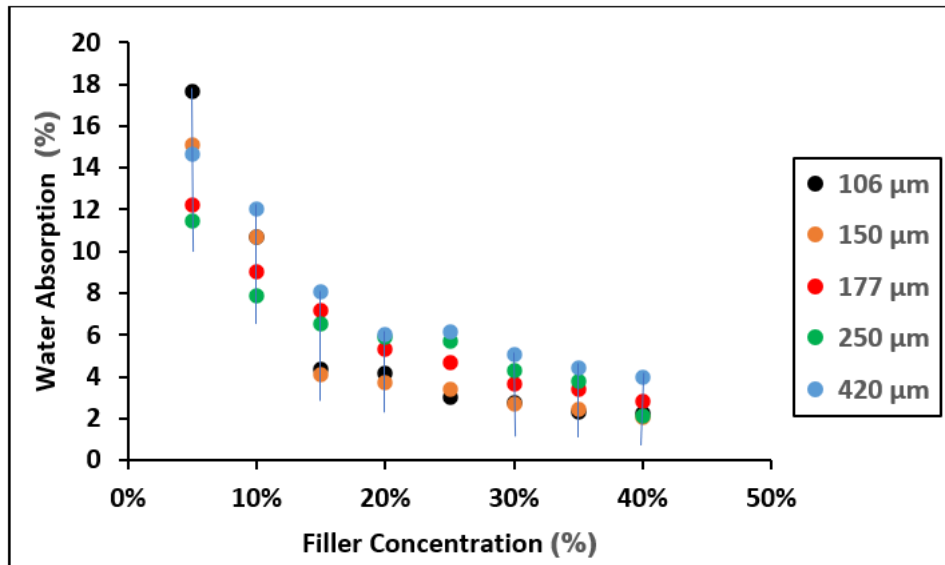


Figure 6a: Mean variance analysis of model one

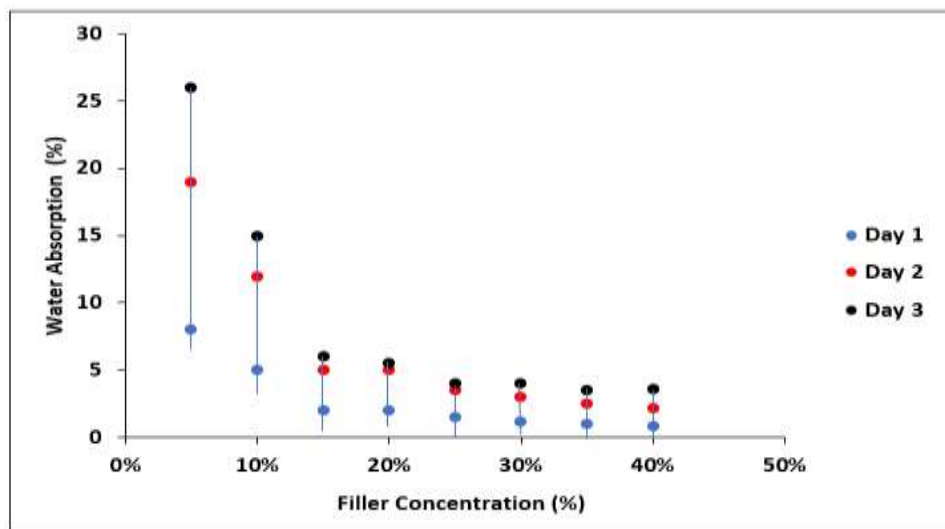


Figure 6b: Mean-variance analysis of model two

3.7 Analysis of Mechanical Properties

3.7.1 Impact energy of the polymer composites

The effect of filler concentration on impact energy is shown in Figure 7. Significantly, all the samples exhibited a similar trend of energy absorption with slight variation in numeric value. A maximum energy absorption value of 21.54 J was recorded in a 150 μm sample at 40 wt. % filler and a minimum energy absorption of 18.38 J in 177 μm sample at 5 wt. % filler. Crystallinity can both enhance and inhibit the interfacial bond between the polymer matrix and the reinforcement, depending on the specific circumstances. The slightly improved energy absorption relates to better filler-matrix interaction at higher filler concentrations and smaller particle sizes. The affinity between the carbonate filler and polymer is key to its fracture resistance and toughness. The existence of a strong bond guarantees effective reinforcement enhancing stress distribution.

The absorbed energy is often dissipated through microcracking and localised deformation. Also, the presence of the amorphous matrix further compensates for the brittleness of the carbonate shell thereby preventing catastrophic failure. The synergy between the plastic matrix and the carbonate shell contributes to the overall toughness of the composite, which is higher than obtainable in pure calcium carbonate crystals. Several studies have also shown that the amount of energy absorbed increases with increases in filler content. This is because higher saturation with filler particles enhances the formation of a more rigid structure that absorbs and dissipates more energy [30, 31].

3.7.2 Ultimate tensile strength (UTS) characteristics of the polymer composites

Figure 8 shows the ultimate tensile strength for all particle sizes. The plot of UTS against filler content did not follow a definite pattern. A peak UTS was attained at different points for various particle sizes and the highest UTS of ~ 1.80 MPa

was observed at 250 μm particle size for 20 wt. % filler content. Generally, the low strength recorded in this work can be attributed to the crystalline nature of the reinforcement which caused the region to be more brittle than the amorphous areas. In some cases, this brittleness can cause micro-cracks or delamination at the interface between the polymer and the reinforcement in conformity with the report of Shirkuma and Dibraka [32].

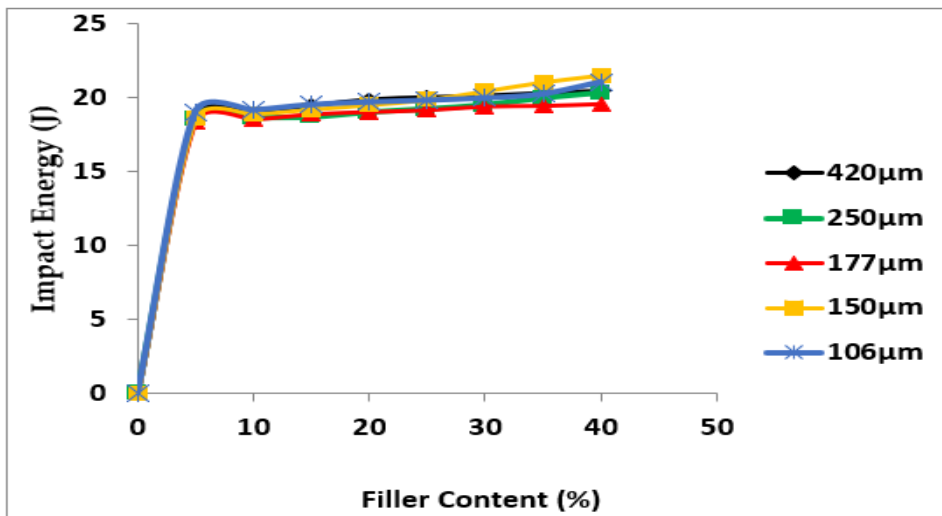


Figure 7: Polyethylene composites' impact energy (J) with filler content for all particle sizes

The sinusoidal profile obtained in this investigation is similar to the UTS pattern reported by Bukar *et al.*, [14] where a low-density polyethylene composite reinforced with coconut fibre was developed with a low tensile strength of 2.2 MPa at 20% filler content. Other complementary experiments by Sasria *et al.*, [12] and Yadvinder *et al.* [13] also recorded low tensile strength and the products recommended for use in applications requiring low strength.

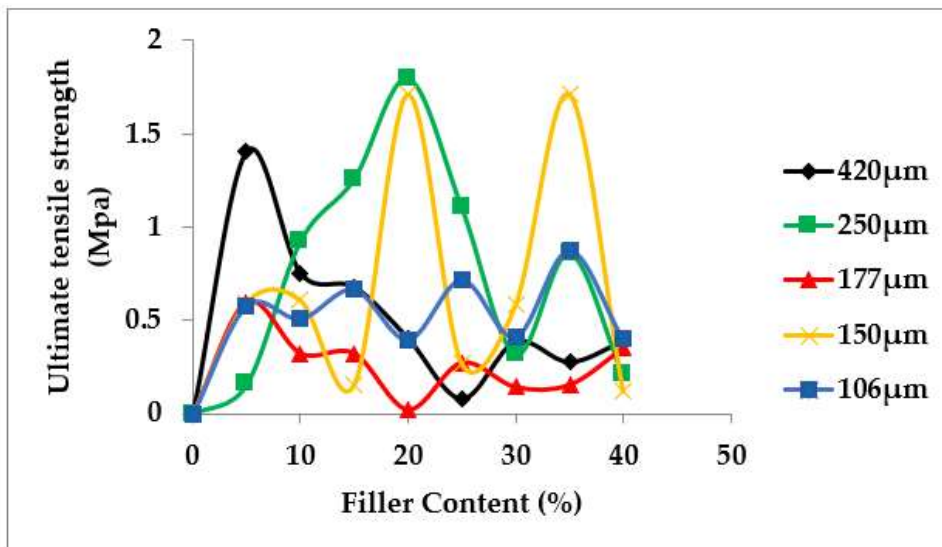


Figure 8: UTS of polymer composites with varied filler concentration

3.7.3 Analysis of ductility property of polymer composites

Figure 9 is a plot of variation ductility with filler concentration. Here, the highest elongation of 42% was obtained in the 106 μm sample at 35 wt. % filler and the lowest elongation of 7% was obtained in the 150 μm sample at 5 wt. % filler. Generally reinforcing polyethylene with a periwinkle shell improves the ductility of the composite. The improvement in elongation could be accredited to a good interface between the reinforcement and the matrix, which allows for craze movement. These induced lattice strains in the composites led to higher strains [33]. The composite that experienced the highest ductility will perform well under tension while the composite that experienced the lowest ductility will perform well under compression.

3.7.4 Flexural strength analysis of polymer composites

Figure 10 revealed that the maximum flexural strength of 11.96 MPa occurred in the 106 μm sample at 5 wt. % filler then drops as filler content increases. The lowest flexural strength of 1.33 MPa was experienced at 250 μm samples at 10 wt. % filler. The flexural strength shows sinusoidal pattern as filler content increases. For the 250 μm sample, the highest

flexural strength of 8.04 MPa was experienced at the 15 wt. % filler contents after which the values dropped as filler content increases. Reduction in flexural strength at the peak of the reinforcements confirms the assumption of controlled mobility of the matrix by filler particles [34].

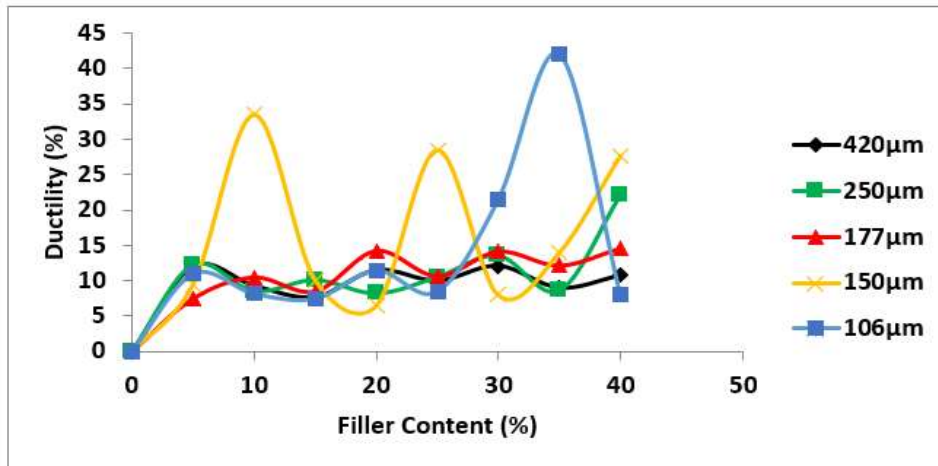


Figure 9: Ductility for composite with varied filler concentration

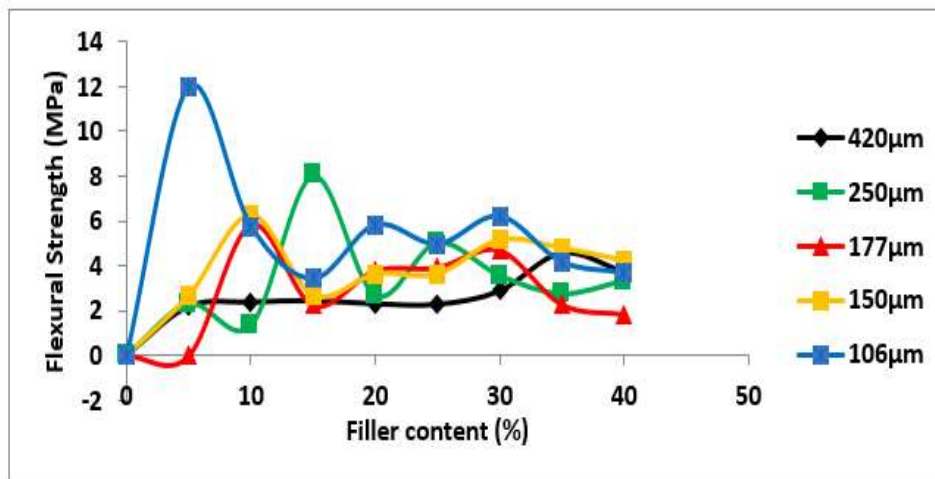


Figure 10: The flexural strength of Polymer composites with varied filler concentration

3.8 Microstructural Investigation

3.8.1 Morphological evaluation of the polyethene composites and virgin periwinkle shell

The morphology of the LDPE as shown in Figures 11 A1, A2, and A3 represents the micrograph of LDPE, pore distribution and 3D intensity respectively. A careful observation of the 3D plot of the micrograph revealed diffuse fibrils matter with very low intensity indicative of an amorphous material. Also, Figures 12 A1, A2 and A3 show the Virgin Periwinkle shell, pores distribution and 3D intensity plot respectively. The morphology exhibited a random orientation of a polycrystalline material. The existence of particle-like feature, is a suggestion that calcium carbonate (CaCO_3), Calcite is present in the material. Further analysis showed that Periwinkle is more porous (41.7%) when compared with LDPE (20%).

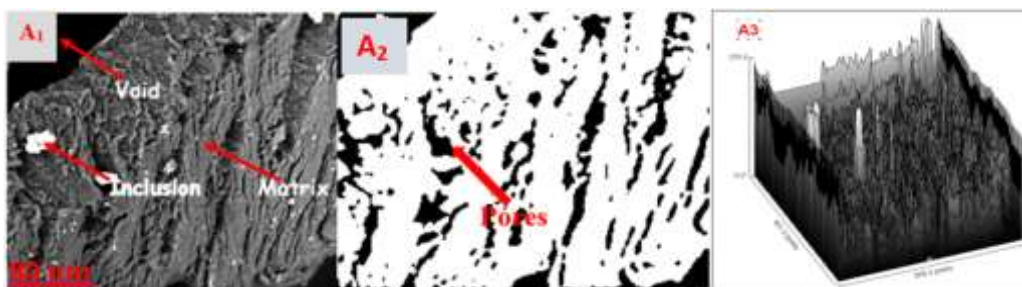


Figure 11: Morphology of unreinforced low-density polyethene

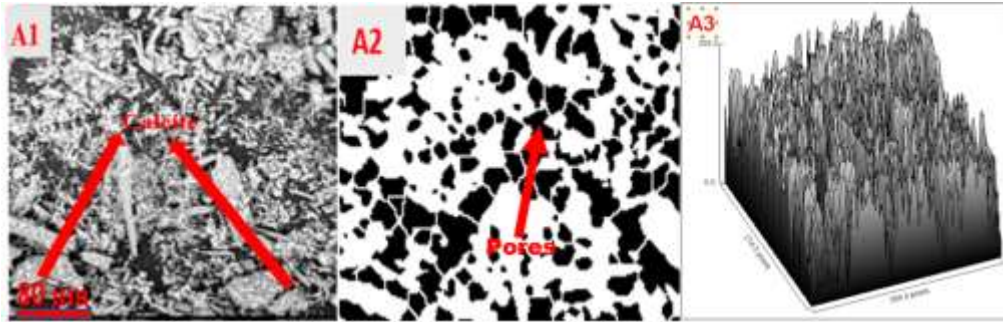


Figure 12: Morphology virgin periwinkle shell

3.8.2 The Morphology of periwinkle reinforced low-density polyethylene (LDPE)

Figures 13-16 show the SEM micrographs of selected polymer composites. Observation shows that the particles were well-wetted by the polyethylene matrix and the composite images with varied constitutions were distinguishable. Specifically, the 106 μm composite filler (Figure 13) achieved a uniform dispersion with no observable pores. It also exhibited good interfacial bonding between the filler and the matrix, with a little agglomeration of filler particles. These features might have accounted for improved ductility and flexural strength reported earlier in section 3.7.4. These support the relatively high mechanical strength shown by the composite [16]. The 3D plot of intensity also revealed a very smooth surface morphology as a result of using finer particles and a high degree of dispersion of filler in the matrix. Notably, the 150, 250 and 420 μm composites in Figures 14 to 16 though having 20 wt. % filler is characterized by a high degree of rough surface and increased void spaces as a result of an increase in particle sizes. This was confirmed by pore analysis carried out with image J software. Deduction, showed that percentage pore for 250 μm , 420 μm , 150 μm , and 106 μm , grade particle sizes are 6.36%, 1.32%, 0.21% and 0.055% pores respectively. Conventionally, larger particle size enhances pores development and uneven surface topography as revealed in subfigure A3 and this has a considerable effect on the absorptivity property of the composite. Conversely, composite constituted from smaller grade particle has a reduced void space, which culminates into a better mechanical property. The micrograph extract, subfigures A2 shows the degree of agglomeration and clustering of floating particles. This feature is of the greatest magnitude in 420 μm 20 wt.% composite, indicative of interfacial bonding, which accounts for the low tensile strength recorded in this research. Agglomeration of particles serves as potential sites for crack propagation [35].

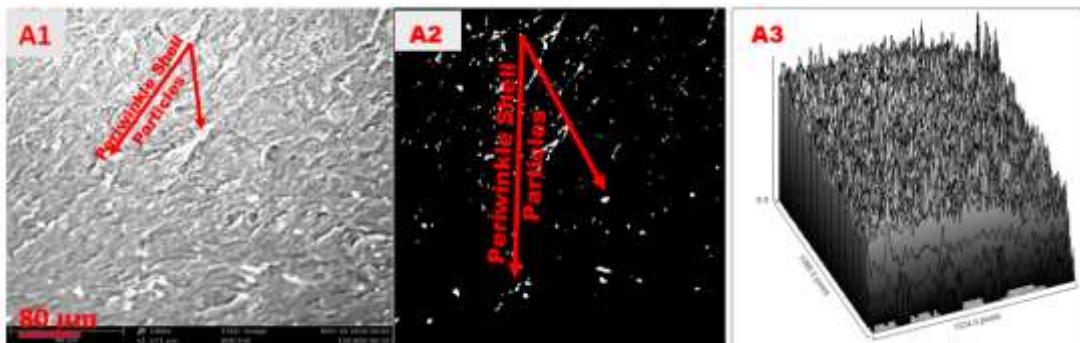


Figure 13: (A1) micrograph of 106 μm 20 wt.% periwinkle shell particle reinforced composite(A2) Distribution of floating Periwinkle Shell particle (A3) 3D intensity

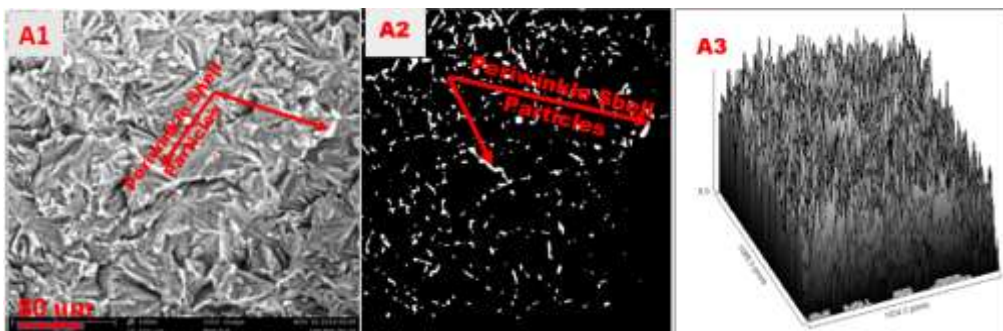


Figure 14: (A1) Micrograph of 150 μm 20 wt.% Periwinkle Shell particle reinforced composite(A2) Distribution of floating Periwinkle Shell particle (A3) 3D intensity

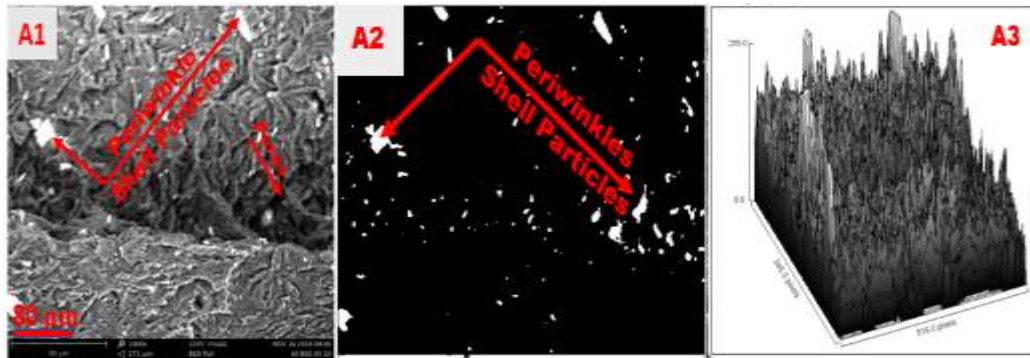


Figure 15: (A1) Micrograph of 250 μm 20 wt.% Periwinkle Shell particle reinforced composite (A2) Distribution of floating Periwinkle Shell particle (A3) 3D intensity

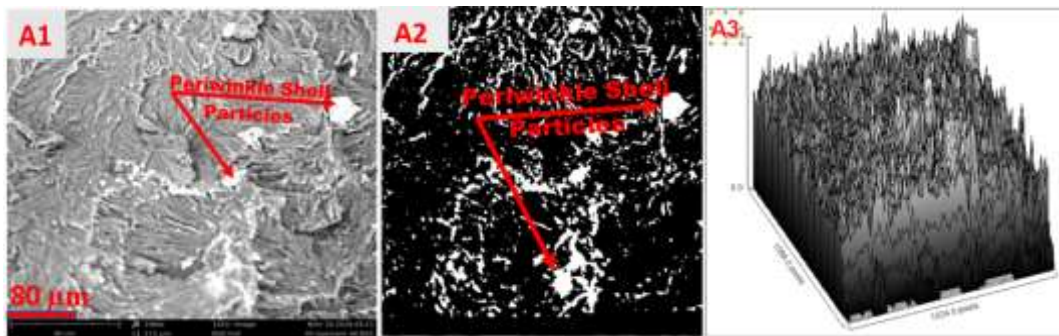


Figure 16: (A1) Micrograph of 420 μm 20 wt.% Periwinkle Shell particle reinforced composite (A2) Distribution of floating Periwinkle Shell particle (A3) 3D intensity

4. CONCLUSION

In this study, the physico-mechanical behaviours of low-density polyethylene reinforced with periwinkle shell particles have been evaluated. The FTIR result indicated a strong presence of CaCO_3 , which enhanced the development of stronger composite material. The concentration and size of the filler content greatly influence the physical and mechanical properties of the periwinkle shell-reinforced composites. Fine-grade particle filler demonstrates good adhesion between matrix and filler particles and uniform dispersion. Specifically, the composite with 106 μm filler at 35% concentration gives superior ductility of 42 % though, with a corresponding minimal UTS value. This makes the developed composite relevant as decorative items or car interiors where flexural strength and ductility are of interest.

Statistical analysis confirmed that water absorption of periwinkle shell-reinforced polyethylene composite decreases with an increase in filler content due to its hydrophilicity. Inference from the mean-variance analysis gave a minimum water absorption value of 4 % for both models one and two. Further deduction from the study revealed that variation in the concentration and size of periwinkle shell filler did not have a significant effect on the ultimate tensile strength of the developed composites.

REFERENCES

- [1] Mark, U., Madufor, I., Obasi, H. & Mark, U. (2019). Influence of filler loading on the mechanical and morphological properties of carbonized coconut shell particles reinforced polypropylene composites. *Journal of Composite Materials*. 54. 002199831985607. [10.1177/0021998319856070](https://doi.org/10.1177/0021998319856070).
- [2] Patel, R.V., Anshul Y., & Jerzy, W. (2023). Physical, Mechanical, and Thermal Properties of Natural Fiber-Reinforced Epoxy Composites for Construction and Automotive Applications. *Applied Sciences* 13(8), 5126. <https://doi.org/10.3390/app13085126>.
- [3] Onuegbu, G. C., & Madufor, I. C. (2012). Effect of filler loadings on the end-use properties of maize tassel filled high density polyethylene. *International Research Journal in Engineering, Science and Technology (IREJEST)*. 9(1), 2.
- [4] Borrero-López, A.M., Concepción, V., & José M. F. (2022). Lignocellulosic Materials for the Production of Biofuels, Biochemicals and Biomaterials and Applications of Lignocellulose-Based Polyurethanes: A Review. *Polymers* 14(5), 881. <https://doi.org/10.3390/polym14050881>.
- [5] Laka, Marianna & Chernyavskaya, Svetlana & Shulga, Galia & Shapovalov, V. & Valenkov, Andrej & Tavroginskaya, Marina. (2011). Use of Cellulose-Containing Fillers in Composites with Polypropylene. *Materials Science*. 17. 10.5755/j01.ms.17.2.484.
- [6] Offiong, U.D., & Godwin, E.A. (2017). Assessment of physico-chemical properties of periwinkle shell ash as partial replacement for cement in concrete. *International journal of scientific engineering and science* 1, (7) 33-36.

- [7] Udo, M., Afolalu, S. A., Ikumapayi, O. M., Babalola, P., Obasa, V., & Akpalikpo, O. (2022). Effect of particle size and weight percentage variation on the mechanical properties of periwinkle shell reinforced polymer (epoxy resin) matrix composite. *International Journal of Applied Science and Engineering*, 19(3), 1-7.
- [8] Omah, A.D., Eze, H.U., Omah, E.C., Ude, S.N., Nwoke, O., Offor, P.O., Njoku, R.E. & Oji, E. (2023). The Effect of Filler Variation and Interfacial Behaviour on the Dielectric Performance of Snail Shell Particulate Polyester Composites. *J. Mater. Environ. Sci.*, 14 (7), 750, 761.
- [9] Omisande, L. A. & Onugba, M. A. (2020). Sustainable Concrete Using Periwinkle Shell as Coarse Aggregate – A Review: *OSR Journal of Mechanical and Civil Engineering (IOSR-JMCE)* 17(6) 17-22. DOI: 10.990/1684-1706031722.
- [10] Adah, P.A., Nuhu, & A.S., Hassan, A. & Ubi, P. (2024). Characterization of periwinkle shell ash reinforced polymer composite for automotive application. 8 (1) 83 - 92. 10.33003/fjs-2024-0801-2158.
- [11] Fakayode, O. A. (2020). Size-based physical properties of hard-shell clam (*Mercenaria mercenaria*) shell relevant to the design of mechanical processing equipment. *Aquacultural Engineering*. 89. 102056. 10.1016/j.aquaeng.2020.102056.
- [12] Sasria, Nia. (2022). Composite Manufacturing of Coir Fiber-Reinforced Polyester as a Motorcycle Helmet Material. *JMPM (Jurnal Material dan Proses Manufaktur)*. 6. 10.18196/jmpm.v6i1.13756.
- [13] Yadvinder. S., Jujhar, S., Shubham, S., Thanh-Danh, L. & Duc-Nam, N. (2020). Fabrication and characterization of coir/carbon-fiber reinforced epoxy based hybrid composite for helmet shells and sports-good applications: influence of fiber surface modifications on the mechanical, thermal and morphological properties. *Journal of Materials Research and Technology*, 9 (6), 15593-15603. <https://doi.org/10.1016/j.jmrt.2020.11.023>.
- [14] Bakar, A., Mohammed, A. & Hammajam, A. (2022). Development and Evaluation of the Mechanical Properties of Coconut Fibre-reinforced Low Density Polyethylene Composite. *Open Journal of Composite Materials*. 12. 83-97. 10.4236/ojcm.2022.123007.
- [15] Juárez-de la, R., Alejandra, B., Muñoz-Saldaña, J., Torres-Torres, D., Ardisson, P. & Alvarado-Gil, Juan. (2011). Nanoindentation characterization of the micro-lamellar arrangement of black coral skeleton. *Journal of structural biology*. 177. 349-57. 10.1016/j.jsb.2011.12.009.
- [16] Odili, C., Gbenedor, O., Adesola, O. & Adeosun, S. (2021). Characterization Of Polylactide (Pla) Composite Reinforced with Biowaste. *Kufa Journal of Engineering*. 12. 119-129. 10.30572/2018/Kje/120208.
- [17] Gbenedor, O. P., Akpan, E. I., & Adeosun, S. O. (2017). Thermal, structural and acetylation behavior of snail and periwinkle shells chitin. *Progress in biomaterials*, 6, 97-111.
- [18] Hajji, S., Turki, T. Boubakri, A., Ben A. M. & Mzoughi, N. (2017). Study of cadmium adsorption onto calcite using full factorial experiment design. *Desalination and Water Treatment*. 83. 222-233. 10.5004/dwt.2017.21079
- [19] Onuoha, C., Onyemaobip, O. Anyakwop, C., Onuegbu, G. & Onuegbu, G. (2017). Physical and Morphological Properties of Periwinkle Shell-Filled Recycled Polypropylene Composites. *IJISSET - International Journal of Innovative Science, Engineering & Technology*, 4. (5), 2348 – 7968.
- [20] Morsch et al. *Organic Chemistry* (2020). Open Education Resource (OER) LibreTexts Project (<https://LibreTexts.org>).
- [21] Shivasharana, C.T. & Sheetal, S.K. (2019). Physical and mechanical characterization of low-density polyethylene and high-density polyethylene. *J Adv Sci Res* 3, 30–34.
- [22] Ibrahim A. & Sylvester G. S. (2015). Assessment of Periwinkle Shells Ash as Composite Materials for Particle Board Production. *International Conference on African Development Issues (CU-ICADI) Materials Technology Track* 158-169.
- [23] Abutu, J.I., Lawal, S., A.I., Ndaliman, M. B.I., Lafia-Araga, R. A. & Abdulrahman A.S (2019). Effects of Particle Size Distribution on the Properties of Natural-Based Composite. *International Journal of Engineering Materials and Manufacture* 4(4) 170-177 <https://doi.org/10.26776/ijemm.04.04.2019.05.3>
- [24] Venkatesh, R. (2024). Synthesis and Behavior Study of Basalt Fiber-Made Low-Density Polyethylene Composites Via Injection Mold. *J. Inst. Eng. India Ser.* <https://doi.org/10.1007/s40033-024-00727-3>.
- [25] Adeosun S.O., Akpan E.I., & Akanegbu H.A. (2015). Thermo-mechanical Properties of Unsaturated Polyester Reinforced Coconut and Snail Shells. *International Journal of Composite Materials* 5(3): 52-64
- [26] Davies, I. E., & Adigio, E. M. (2022). Effect of Periwinkle Shell on the Physical and Mechanical Properties of Sandcrete Block. *Nigerian Journal of Technological Research*, 17(1), 46-54.
- [27] Elbishari, H., Silikas, N. & Satterthwaite, J. (2012). Filler size of resin-composites, percentage of voids and fracture toughness: Is there a correlation?. *Dental materials journal*. 31. 523-7. 10.4012/dmj.2011-256.
- [28] Satish, K., Shejkar, B. A., & Alok A., (2021). Effect of particle size on physical properties of epoxy composites filled with micro-size walnut shell particulates, *Materials Today: Proceedings*, 47(11), 2657-2661. <https://doi.org/10.1016/j.matpr.2021.02.520>.
- [29] Mishra, P., Pandey, C. M., Singh, U., Gupta, Anshul, S. & Chinmoy, K.A. (2019). Descriptive Statistics and Normality Tests for Statistical Data. *Annals of Cardiac Anaesthesia* 22(1), 67-72. | DOI: 10.4103/aca.ACA_157_18
- [30] Bhanu P.N. & Madhusudhan T. (2015). Investigative study on impact strength variation in different combination of polymer composites. *International Journal of Engineering Research and General Science*, 3, 306–312.

- [31] Akhyar, A.G., Masri, I., Fatlul, U. & Ahmad, F. (2024). The influence of different fibre sizes on the flexural strength of natural fibre-reinforced polymer composites, *Results in Materials*, 21. <https://doi.org/10.1016/j.rinma.2024.100534>
- [32] Shvkakumari, P. & Dibakar, B. (2017). Effect of red mud on mechanical and chemical properties of unsaturated polyester-epoxy-bamboo fiber composite. *Mater Today: Proceeding* 4(33),25-33
- [33] Bennerth, N.N. (2012). Microstructure And Mechanical Properties of Epoxy-Rice Husk Ash Composite | University of Nigeria, Nsukka Open Education Resources (OER).
- [34] Ofem, M. I. & Umar, M. (2012). Effect of filler content on the mechanical properties of periwinkle shell reinforced CNSL resin composites. *ARPN Journal of Engineering and Applied Sciences*, 7(2), 212-215.
- [35] Tazibt, N., Kaci, M., Dehouche, N., Ragoubi, M., & Atanase, L. I. (2023). Effect of filler content on the morphology and Physical Properties of Poly (Lactic Acid)-Hydroxyapatite Composites. *Materials*, 16(2), 809. <https://doi.org/10.3390/ma160208>.